Second Conference on Smart Monitoring,
Assessment and Rehabilitation of Civil Structures

SMAR 2013

Wireless monitoring of the dynamic performance of a footbridge

Kallirroi Flouri[1], Reinhard Bischoff[2], Jonas Meyer[2] and Glauco Feltrin[1]

[1] Empa, Swiss Federal Laboratories for Materials Science and Technology, Structural Engineering Laboratory, Duebendorf , Switzerland
[2] Decentlab GmbH, Duebendorf , Switzerland

ABSTRACT: Monitoring the dynamic performance of structures usually requires a deployment of several weeks or months to collect a data set allowing a reliable assessment. Since for this type of medium term deployments installation costs are a key factor, wireless monitoring with its fast deployment has an advantage over wired monitoring systems. This paper describes a deployment of a wireless monitoring system on a timber footbridge. The goal of the monitoring was to provide information about vibration amplitudes during operation and to track the changes of relevant natural frequencies with temperature. The monitoring data quality matched the requirements of a dynamic performance assessing process. The wireless monitoring system worked for about one year with very high reliability. Battery replacement was necessary only once after 6 months of operation. The deployment demonstrated that a wireless sensor network is a technically feasible and economically effective mean to monitor the dynamic performance of a structure.

1 INTRODUCTION

Excessive vibration of civil structures such as footbridges, floors, staircases etc. may produce discomfort for the users and, as a consequence, may lead to a restricted use or a retrofitting of the structure. By far the most famous case of excessive vibrations of the last years was the Millenium Bridge in London which under crowd loading on its opening day exhibited such high lateral vibrations that the bridge had to be closed and retrofitted (Dallard et al. (2001)). To prevent such cases, design codes specify design rules usually in terms of natural frequencies and vibration amplitude limits.

Despite the fact that the excitation process by pedestrians is random, only recently attempts have been made to develop probabilistic concepts for defining vibration serviceability. Based on observations of the perception of pedestrians to the vibrations amplitudes of a pedestrian bridge, Kasperski (2006) developed a serviceability criterion for pedestrians exposed to vibrations. He proposed a tentative serviceability limit in terms 1s RMS value of accelerations that is 2.5 time lower than the limit of the ISO 10137 (2007), the most recent code in this area. By interviewing pedestrians about the vibration perceived during normal traffic on a lively footbridge, Zivanovic & Pavic (2009) proposed a serviceability criterion based on a conditional probability function that allows to estimate the percentage of people feeling unhappy during the usage of a footbridge. A probabilistic serviceability assessment methodology requires a monitoring of the bridge vibrations over a reasonable long period of time. Hu et al. (2012) presented recently a study on long term vibration monitoring of a footbridge. They investigated the variation of natural frequencies and damping ratios induced by temperature and pedestrian traffic and the occurrence frequency of maximum daily lateral and vertical accelerations.

In all these studies, monitoring was performed with a conventional wired instrumentation. Wired monitoring systems are reliable, accurate but costly in terms of instrumentation and deployment. Wireless sensor networks (WSNs) have emerged as an alternative structural monitoring tool. By using less accurate sensors and due to the wireless communication, WSNs have the potential to significantly reduce the monitoring cost. On the other hand, sensor nodes have restricted communication and computation capabilities since they are powered by batteries. To achieve long-term deployment periods, the raw data needs to be processed in the nodes in order to reduce the amount of data for transmission. Since in general data processing requires less energy than data transmission, the battery replacement period of a node can be extended.

In this paper we explore the performance of a WSN for vibration serviceability monitoring of a timber footbridge. The monitoring, which lasted for more than a year, addresses the impact of temperature changes on natural frequencies and vibration amplitudes. The ambient as well as pedestrian induced vibrations of the footbridge were recorded permanently and natural frequencies as well as the envelope of vibration amplitudes were computed by in-node data processing.

2 WIRELESS SENSOR NETWORK

2.1 Hardware

The sensor node is based on the commercial Tmote Sky WSN platform (Polastre et al. (2005)). This platform is well suited for long term deployments because of its very low power consumption (5.4mW at radio-off state and 65mW at full operational mode). The vibrations are captured with the LIS3L02 capacitive MEMS acceleration sensor of ST Microelectronics. It can be operated in a bandwidth of 0-2kHz with an amplitude range of ±2g and a sensitivity of 0.6V/g, which is a quite good performance for such a low cost product.

The signal conditioning unit had an analogue amplification and filtering circuit. Both circuits are implemented using a low-power amplifier. The filtering circuitry consisted of a 1st-order high-pass and two 2nd-order low-pass Butterworth filters. The high-pass filter was implemented to remove the DC sensor signal component due to gravitation. This DC filtering allows to increase the amplification range of the AC acceleration signal. The amplifier magnified the signal 50 times such that the amplitude range of the signal was limited to $\pm 0.481 ms^{-2}$. The low-pass filter was used as anti-aliasing filter with a cut-off frequency of 20Hz. The resolution of acceleration sensing is given by the theoretical noise level of the accelerometer which was about 0.25mg rms ($0.0025 ms^{-2}$). To avoid a bias of the vibration amplitude signal with voltage drop because of energy consumption, the sensor node is equipped with a voltage regulator that provided the accelerometer with a constant input voltage of 3V. Ambient temperature and humidity were measured with the single chip Sensirion SHT11 sensor.

2.2 Software

The sensor node software is called STONE and it is described in detail in Flouri et al. (2012). Here we summarize the most relevant features. The sensor node software builds on TinyOS version and consists of two program images, the reprogramming image and the monitoring image, which are stored in the external flash memory, Figure 1. The reprogramming image, which is used for updating the monitoring image, is a modified version of Deluge (Hui & Culler (2004)) and allows reprogramming each sensor node individually over the air. Except for the root node, all sensor nodes use the same reprogramming image. The monitoring image is specifically tailored to each sensor node depending on the set of physically attached sensors and

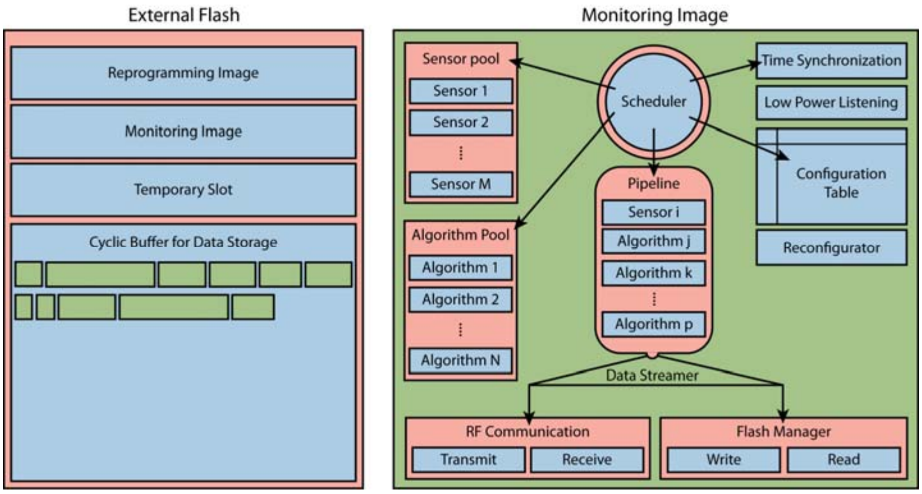

Figure 1: Software architecture of STONE.

in-node data processing. This mechanism allows minimizing the size of the monitoring image. It includes the software to access the sensor data, the processing algorithms to extract relevant information, which is transmitted to the base station, a time synchronization protocol and a scheduler that executes measurement tasks. The final step of each measurement and data processing task is to route the output data of the pipeline either to the communication module or to the flash manager.

3 FOOTBRIDGE AND MONITORING SET-UP

The timber footbridge Städtlisteg in Mellingen, Switzerland, is a three span bridge with a total length of 58m and a width of 2.5m, Figure 2a). The spans have widths of 18, 22 and 18m. The mid-span has two joints. Each joint is located at a distance of 3.8m from the supports. The bridge section is composed of four glued-laminated timber girders with a height of 633mm and a width of 200mm. The deck is made of cross-laminated solid timber panels with a width of 2.5m and a thickness of 85mm. These panels are glued on top of the girders. The asphalt pavement was deployed in two layers directly on top of the cross-laminated solid timber panels and has a thickness of 35mm.

The design of the bridge was governed by the vibration serviceability. The design goal was to achieve a fundamental frequency between 2.5 and 3.5Hz. This choice would allow avoiding the frequency ranges of pedestrian’s step frequency (1.7…2.4Hz) and its second harmonic (3.5…4.5Hz). Depending on the assumptions about the material property of the timber

a)  b) 

Figure 2: a) Lateral view of the footbridge. b) Mounting of a sensor node.

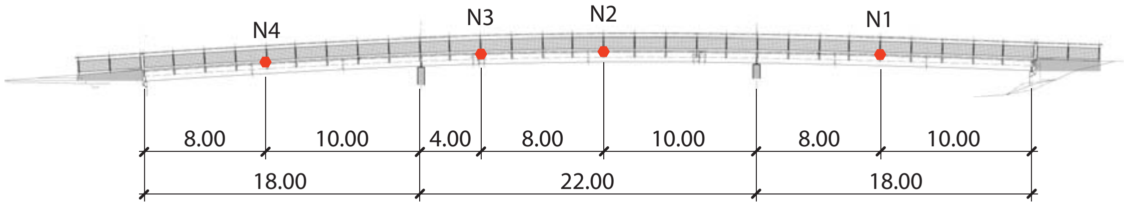

Figure 3: Elevation view of the footbridge with the mounting positions of the sensor nodes.

components, the fundamental frequency of the bridge was estimated by the designer to be in the range of 2.6 to 2.85Hz (Fuhrmann (2000)). Vibration measurements showed that natural frequencies and modal damping ratios change with temperature. These changes are induced by the asphalt pavement since the storage and loss modulus of the mastic asphalt varies by orders of magnitude if the asphalt temperature changes from -20° to 50°C.

The deployment consisted of 4 sensor nodes, 1 relay node and a basis station. The 4 sensor nodes were mounted on the footbridge below the bridge deck on the support pole of the handrail (Figure 2b and Figure 3). The base station was powered by the mains supply within a house 50m from the bridge. Since a house was situated between the base station and the sensor nodes, a relay node was placed on a pole of the public lighting to improve the link quality between sensor nodes and base station. The sensor nodes N1 and N2 were recording the vibration amplitudes and the sensor nodes N3 and N4 the natural frequencies. In addition, each node measured temperature, humidity and supply voltage with a period of 15 minutes. The monitoring system was deployed in one and a half hours.

4 IN-NODE DATA PROCESSING

4.1 Calculation of vibration amplitude

We calculate the envelope from the recorded data since the greatest amplitude of a record corresponds to the greatest amplitude of the envelope (Figure 4). After recording the raw data, the maximum amplitude is compared to a given threshold. If the threshold is not exceeded the recorded raw data is overwritten by a subsequent data record. If the threshold is exceeded, the recorded data is pipelined to the next processing step and the envelope of the vibration record is computed. The recording time period is split up into segments with a constant time interval. Within each of these time intervals the smallest and the greatest vibration amplitude is determined. Obviously, the coarser the time interval the most effective is the data reduction.

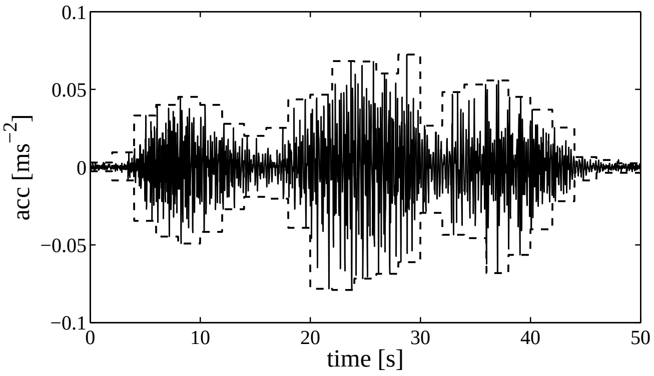

Figure 4: Peak amplitude envelope of vibration recording with a time interval of 2s.

4.2 Calculation of natural frequencies

Many methods exist for estimating natural frequencies from vibration records. The most common is probably based on the picking of peaks of an averaged frequency spectrum. Averaging improves the estimation of the spectrum by reducing the impact of random noise on the estimation of natural frequencies by pick picking. Because of the limited data storage capabilities, however, averaging is cumbersome and inefficient to implement in a WSN node. In addition, peak picking is not unproblematic since usually it is done manually and therefore subjected to a significant degree of subjectivity. Automated peak picking algorithms for natural frequency estimations have been investigated by Lynch et al. (2006), Zimmerman et al. (2008), Feltrin et al. (2009) and Lei et al. (2010). In these studies, no long term tests were performed to assess the performance of the algorithms. Because of noise, a single natural frequency estimation may be inaccurate. However, by analyzing a large sample of such single records we expect to obtain a more accurate estimate of a natural frequency by calculating the average of the sample. This post-processing can be done effectively at the backend, thus reducing the complexity of the WSN node software. The algorithm, which was very briefly described in Flouri et al. (2012), was previously tested in a long term deployment for monitoring the natural frequencies of cable stays. The natural frequencies estimation is performed in 6 steps and demonstrates very well the data processing pipeline of the sensor node software.

5 RESULTS

5.1 Vibration amplitude

Figure 5a) displays an envelope recorded by node N2, which was placed in the midspan of the center span. As expected, the maximum vibration amplitude was achieved when the excitation source was moving on the center span. In this case, the envelope allows us to estimate the speed of the excitation source. Since the vibration period was about 18 seconds, the speed of the source was approximately 11 km/h. This speed suggests that the vibrations were probably induced by a jogger than a pedestrian that was walking over the bridge.

The occurrence frequency of maximum vibration amplitude can be investigated with the empirical probability distribution function (pdf) of the amplitude peak of the records (Figure 5b). The histogram shows that the most likely peak vibration amplitude is about 0.05 ms^{-2}. Furthermore, at node 2, in the midspan of the center span, great peak amplitudes are more likely to occur than at node 1, which is placed on a lateral span.

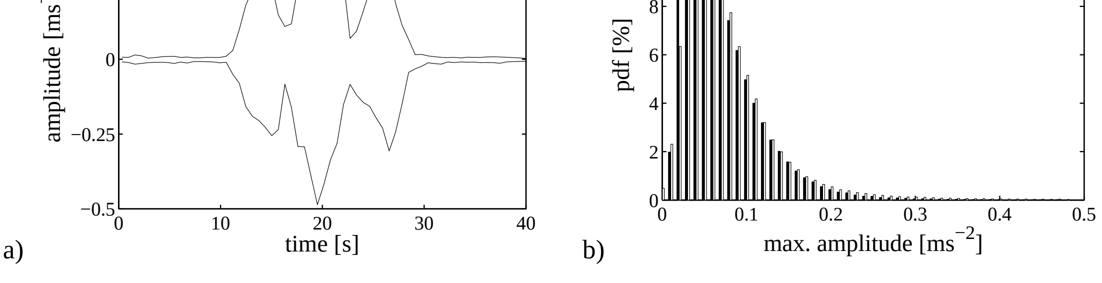

Figure 5: a) Envelope of vibration amplitudes recorded at node N2. b) Histogram of the empirical probability distribution functions of peak vibration amplitudes of nodes N1 and N2.

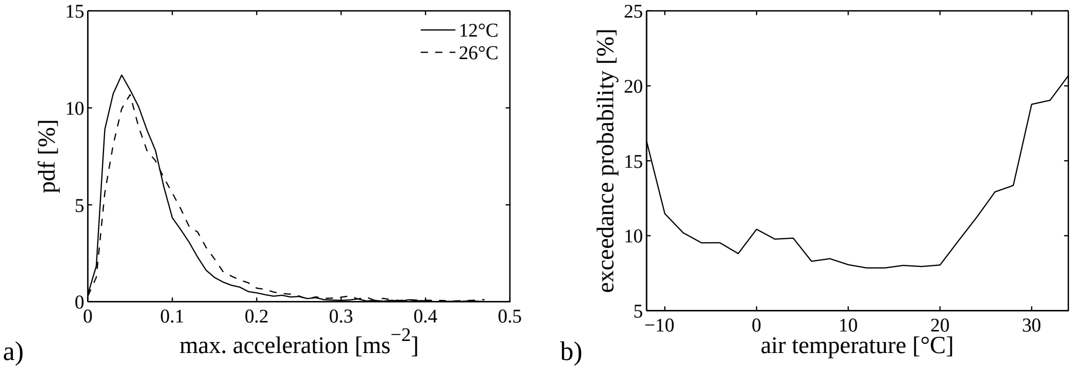

Figure 6: a) Histogram of the empirical probability distribution functions of the maxima of the vibration amplitude of node N2. b) Probability of exceeding the peak amplitude of $0.15ms^{-2}$.

To analyze the relationship between vibration amplitudes and temperature, each envelope record was linked to an air temperature using the time stamp of the record. Afterwards, these temperatures were used to associate each envelope record to one of the 24 temperature classes that resulted from subdividing the temperature range between -13°C and 35°C into intervals with width of 2°C. Finally, the peak amplitudes of the records within a temperature class were used to construct empirical probability distribution functions of peak amplitudes.

Figure 6a) shows the difference between the empirical pdf associated to 12°C and 26°C respectively. The pdf at 26°C has higher amplitudes than the pdf of 12°C for peak acceleration greater than 0.09 ms^{-2} and smaller amplitudes below this peak acceleration. This effect is even more pronounced when analyzing the tail of the empirical pdfs at different air temperatures. Figure 6b) displays the probability of exceeding the peak amplitude of $0.15ms^{-2}$ at different air temperatures. The diagram depicts a much higher exceedance probability at air temperatures higher than 20°C.

5.2 Natural frequencies

The natural frequencies were estimated using data records with 2048 samples. Since the sampling rate was 50Hz the time span of a record was 40.96 s. A small pause of approximately 5 seconds was inserted between two subsequent data records. The data acquisition was thus nearly permanently. Figure 7a) displays the computed natural frequencies over a period of two days. The plot shows two clearly distinguishable curved bands that correspond to the natural frequencies of the 1^{st} and 2^{nd} bending modes.

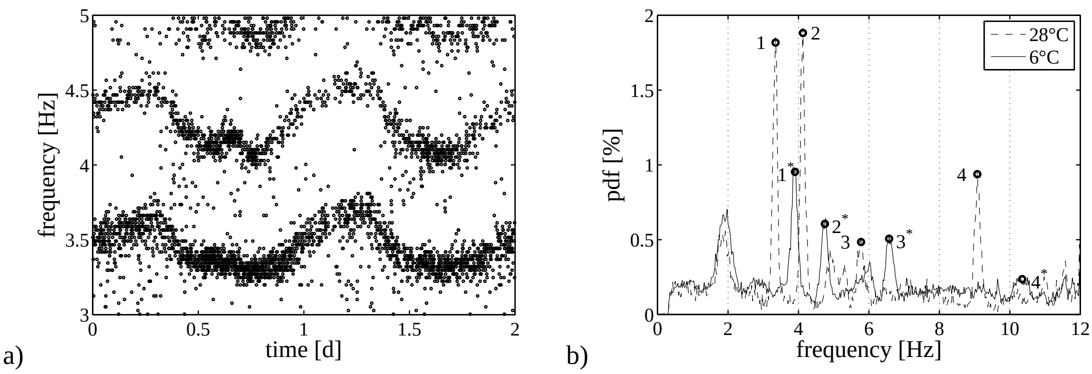

Figure 7: a) Natural frequency estimations. b) Occurrence distribution of natural frequency estimations at node 3 at air temperature of 6°C and 28°C.

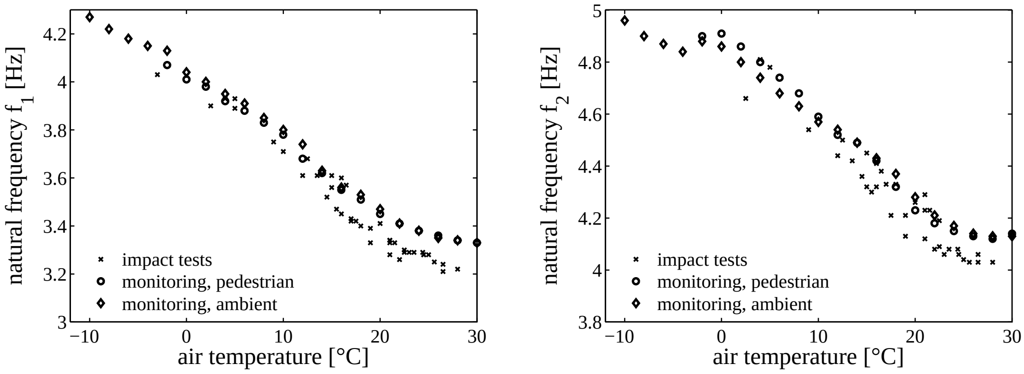

Figure 8: Relationship between natural frequencies and air temperature of the first and second bending mode.

To analyse the impact of temperature on natural frequencies, each frequency record was associated to an air temperature by using the procedure described in the previous section. For a specific temperature interval, the natural frequencies were estimated by analyzing the empirical pdfs of natural frequency estimations. Since natural frequencies have a high probability of being identified by the algorithm, the pdfs should display isolated peaks at the location of natural frequencies. Figure 7b) displays significant isolated peaks at the location of natural frequencies for temperature values of 6°C and 28°C.

Figure 8 displays the changes of natural frequencies of the first and second vibration modes over the complete temperature range. It also displays the natural frequencies that were determined with independent measurements. These measurements were performed at different days with wired high resolution accelerometers and the vibrations were recorded with a 24bit signal acquisition device. The natural frequencies were estimated using the responses of impact tests (person jumping on the bridge) and they agree quite well with the natural frequencies that resulted from monitoring. At air temperatures above 15°C, the impact tests show natural frequencies that are a little bit smaller than those obtained from monitoring. This gap is due to the nonlinear behavior of the timber bridge that displayed a reduction of natural frequencies with increasing vibration amplitudes.

6 CONCLUSIONS

This paper investigates the performance of a WSN for vibration serviceability monitoring of a timber footbridge. Despite the mediocre sensitivity of the MEMS accelerometer and the limitations of the 12bit ADC, the natural frequency estimations obtained from ambient vibration records are in good agreement with independent vibration tests. The monitoring of peak amplitudes could be performed with a significantly simpler algorithm as the monitoring of natural frequencies. Power efficiency could be improved by discarding vibration records containing ambient vibration. The vibration data were processed to empirical probability density functions of peak amplitudes which can be used as basis for a vibration serviceability assessment. The field test demonstrated that a WSN monitoring system can be a technically feasible and economically effective mean to monitor the dynamic performance of a structure.

7 ACKNOWLEDGEMENTS

The authors express their gratitude to the Fonds zur Förderung der Wald- und Holzforschung dof the Federal Office for the Environment, the Swiss Federal Roads Office, and the directory board of Empa for the financial support.

8 REFERENCES

ISO 10137. 2007. Bases for design of structures - serviceability of buildings and walkways against vibrations. International Organization for Standardization.

Dallard, P., Fitzpatrick, A. J., Flint, A., Le Bourva, S., Low, A., Ridsdill-Smith, R. M., & Willford, M. R. 2001. The london millennium footbridge. *Structural Engineer*, 79(22): 17–33.

Feltrin, G., Meyer, J., Bischoff, R., & Motavalli, M. 2009. Modular low-power wireless sensor network for structural health monitoring. *4th International Conference on Structural Health Monitoring on Intelligent Infrastructure (SHMII-4) Zurich, Switzerland, 22-24 July 2009*, on CD.

Flouri, K., Saukh, O., Sauter, R., Jalsan, K. E., Bischoff, R., Meyer, J., & Feltrin, G. 2012. A versatile software architecture for civil structure monitoring with wireless sensor networks. *Smart Structures and Systems*, Vol. 10(3): 209-228.

Fuhrmann, C. 2000. Timber bridge over the reuss river in mellingen, switzerland. *Structural Engineering International (IABSE)*, 10(3): 152-154.

Hu, W.-H., Moutinho, C., Caetano, E., Magalhães, F., & Cunha, Á. 2012. Continuous dynamic monitoring of a lively footbridge for serviceability assessment and damage detection. *Mechanical Systems and Signal Processing*, 33: 38-55.

Hui, J. W., & Culler, D. 2004. The dynamic behavior of a data dissemination protocol for network programming at scale. In (eds), *Proceedings of the 2nd international conference on embedded networked sensor systems*, Baltimore, MD, USA.

Kasperski, M. 2006. Vibration serviceability for pedestrian bridges. *Proc. Instit. Civil Eng.: Struct. Build.*, 159(5): 273–282.

Lei, Y., Shen, W. A., Song, Y., & Wang, Y. 2010. Intelligent wireless sensors with application to the identification of structural modal parameters and steel cable forces: From the lab to the field. *Advances in Civil Engineering*, 2010.

Lynch, J. P., Yang, W., Loh, K. J., Jin Hak, Y., & Chung Bang, Y. 2006. Performance monitoring of the geumdang bridge using a dense network of high-resolution wireless sensors. *Smart Materials and Structures*, 15(6): 1561-75.

Polastre, J., Szewczyk, R., & Culler, D. 2005. Telos: Enabling ultra-low power research. *Information Processing in Sensor Networks/SPOTS, Berkeley (CA) April*.

Zimmerman, A. T., Shiraishi, M., Swartz, R. A., & Lynch, J. P. 2008. Automated modal parameter estimation by parallel processing within wireless monitoring systems. *Journal of Infrastructure Systems*, 14(1): 102-113.

Zivanovic, S., & Pavic, A. 2009. Probabilistic assessment of human response to footbridge vibration. *J. Low Freq. Noise Vib. Active Contr.*, 28(4): 255–268.